Eur. Phys. J. B **14**, 19–28 (2000)

THE EUROPEAN PHYSICAL JOURNAL B

EDP Sciences

Dynamical mean-field theory of a simplified double-exchange model

B.M. Letfulov[a]

Institute of Metal Physics, Ural Division of Russian Academy of Sciences, Kovalevskaya str. 18, Yekaterinburg, 620219 Russia

Received 28 May 1999 and Received in final form 14 July 1999

Abstract. Simplified double-exchange model including transfer of the itinerant electrons with spin parallel to the localized spin in the same site and the indirect interaction J of kinetic type between localized spins is comprihensively investigated. The model is exactly solved in infinite dimensions. The exact equations describing the main ordered phases (ferromagnetic and antiferromagnetic) are obtained for the Bethe lattice with $z \to \infty$ (z is the coordination number) in analytical form. The exact expression for the generalized paramagnetic susceptibility of the localized-spin subsystem is also obtained in analytical form. It is shown that temperature dependence of the uniform and the staggered susceptibilities has deviation from Curie-Weiss law. Dependence of Curie and Néel temperatures on itinerant-electron concentration is discussed to study instability conditions of the paramagnetic phase. Anomalous temperature behaviour of the chemical potential, the thermopower and the specific heat is investigated near the Curie point. It is found for $J = 0$ that the system is unstable towards temperature phase separation between ferromagnetic and paramagnetic states. A phase separation connected with antiferromagnetic and the paramagnetic phases can occur only at $J^* > J^* \simeq 0.318$. Zero-temperature phase diagram including the phase separation between ferromagnetic and antiferromagnetic states is given.

PACS. 71.10.Fd Lattice fermion models (Hubbard model, etc.)

1 Introduction

Double exchange (DE) is one of the forms of indirect exchange interaction between the localized magnetic moments *via* itinerant electrons [1–4]. Historically, it arose in connection with experimental study of the hole-doped manganese oxides $La_{1-x}M_xMnO_3$, where M = Sr, Ca, Ba or Pb [5], and with the ascertainment of the close connection between electric and magnetic properties of these substances (for a review see Ref. [6]).

Usually, the double-exchange mechanism is considered in the frame of the $s-f$ (or $s-d$) model which was first defined by Vonsovskii in 1946 [7]. The Hamiltonian of the $s-f$ model in the Wannier representation has the form

$$\mathcal{H} = \sum_{\langle ij\rangle\sigma} t_{ij} a^\dagger_{i\sigma} a_{j\sigma} - I \sum_{i\sigma\sigma'} (\mathbf{S}_i \mathbf{s})_{\sigma\sigma'} a^\dagger_{i\sigma} a_{i\sigma'} \qquad (1)$$

where $\mathbf{S}_i$ is the operator of localized spin at the site with number i, $\mathbf{s}$ are the Pauli matrices, $a_{i\sigma}$ is the annihilation operator of itinerant electron with the spin projection σ in the i-th site, t_{ij} is the transfer integral ($t_{ij} = t_{ji}$) and I denotes the intraatomic exchange interaction between localized and itinerant electrons. It is assumed that $I > 0$.

A main feature of the double-exchange mechanism is the rigorous parallelism (or antiparallelism in the case of $I < 0$) of the localized and the itinerant-electron spins in the same site. The ferromagnetic ordering is possible only at this condition. It is easy to see that double occupation of the magnetic site by itinerant electrons is excluded in this case. Therefore, the double-exchange mechanism is realized in the $s-f$ system at the limit $I \to \infty$, and the effective Hamiltonian of double exchange presents the transfer process of an itinerant electron from one singly occupied site j to another unoccupied site i with the spin parallel to the localized spin at either site:

$$\mathcal{H}_{\rm dex} = \sum_{\langle ij\rangle\sigma} t_{ij} c^\dagger_{i\sigma} c_{j\sigma} \qquad (2)$$

where $c_{i\sigma}\left(c^\dagger_{i\sigma}\right)$ is the annihilation (creation) operator of the itinerant electron with the spin parallel to the localized spin. In quantum case, this operator looks like [4]

$$c_{i\sigma} = \sum_{\sigma'} \left(P^+_i\right)_{\sigma\sigma'} (1 - a^\dagger_{i-\sigma'} a_{i-\sigma'}) a_{i\sigma'} \qquad (3)$$

where

$$\left(P^+_i\right)_{\sigma\sigma'} = \frac{(S+1)\delta_{\sigma\sigma'} + (\mathbf{S}_i \mathbf{s})_{\sigma\sigma'}}{2S+1} \qquad (4)$$

is the projection operator to the state of an electron at the i-th site with the spin parallel to the localized spin.

[a] e-mail: Barri.Letfulov@imp.uran.ru

In the case of the classical localized spins, where $\mathbf{S}_i = (\sin\theta_i\cos\varphi_i, \sin\theta_i\sin\varphi_i, \cos\theta_i)$, $c_{i\sigma}$ has the form

$$c_{i\sigma} = \frac{1}{2}\sum_{\sigma'}\{\delta_{\sigma\sigma'} + (\mathbf{S}_i\mathbf{s})_{\sigma\sigma'}\}a_{i\sigma'}. \quad (5)$$

Using the transformation [8]

$$b_i = \cos\frac{\theta_i}{2}a_{i\uparrow} + \sin\frac{\theta_i}{2}\mathrm{e}^{-\mathrm{i}\varphi_i}a_{i\downarrow}, \quad (6)$$

we obtain a system of the spinless fermions [9]

$$\mathcal{H}_{\mathrm{dex}} = \sum_{\langle ij\rangle}\tilde{t}_{ij}b_i^{\dagger}b_j \quad (7)$$

with the effective transfer integral

$$\tilde{t}_{ij} = t_{ij}\left(\cos\frac{\theta_i}{2}\cos\frac{\theta_j}{2} + \sin\frac{\theta_i}{2}\sin\frac{\theta_j}{2}\mathrm{e}^{-\mathrm{i}(\varphi_i-\varphi_j)}\right). \quad (8)$$

It should be noted that $\mathcal{H}_{\mathrm{dex}}$ with $c_{i\sigma}$ from (3) (see Ref. [4]) has a complicated mathematical structure, and correct investigation of DE with the help of this Hamiltonian is very difficult task. Therefore, theoretical study of DE is carried out, in the main, either on the basis of the Hamiltonian (1) at the limit $I \to \infty$ or in the frame of the Hamiltonian (7) (often without Berry phase).

For the system with the Hamiltonian (1), the more important results were obtained with the help of different computational techniques (the Monte-Carlo method, the Lanczos algorithm, the density-matrix renormalization-group method). In particular, it was shown [10–13] that phase diagram has three dominant regions: (i) a ferromagnetic phase, (ii) phase separation between hole-poor antiferromagnetic and hole-rich ferromagnetic states, and (iii) a phase with incommensurate spin correlations. The regime of phase separation was discussed with possible experimental consequences for the manganese oxides.

For investigation of systems with the Hamiltonian (7), the various versions of static mean-field approximation were offered [14–23]. The basis of these versions is a decoupling procedure of the Hartree-Fock type with different modifications taking account of the features of considered system. On the whole, we have a few contradictory results which give different numerical estimates of the same physical quantities (for example, for the Curie temperature of the pure DE system).

It should be noted in connection with it that mean-field approximation for strongly correlated electron systems is not trivial and it is not identical to the Hartree-Fock approximation. These approximations are identical for systems with intersite interaction of Coulomb or exchange type (the Heisenberg model, the model of interacting spinless fermions [24]). As the mean-field approximation is exact for the mentioned models in infinite-dimensional space and hypercubic crystals with the infinite number of nearest neighbours, there is opinion that correct mean-field approximation for the strongly correlated electron systems arises at exact solution of the corresponding models in infinite dimensions and subsequent utilization of obtained solution for real systems. Approximation obtained by this way does not take account of spatial fluctuations but it contains dynamical fluctuations. Therefore, it is called the dynamical mean-field approximation.

The foundation of the theory of strongly correlated systems in infinite dimensions was developed in the papers of Metzner, Vollhardt [25] and Müller-Hartmann [26] (for a review see Refs. [27,28]). Furukawa [29,30] has used these ideas for a development of a theory of the manganese oxides on the basis of the Hamiltonian (1) with the classical localized spins ($S \to \infty$). He has shown that a more accurate calculation of some physical quantities gives a good agreement with experimental data. In particular, the accurate treatment of the model (1) gives a suppression of the ferromagnetic transition temperature T_{K} in contrast with the estimate of T_{K} in reference [14]. Moreover, Furukawa has concluded that the DE alone explains the main physical properties (in particular, magnetoresistance) of $\mathrm{La}_{1-x}\mathrm{Sr}_x\mathrm{MnO}_3$, and LSMO is a canonical DE system (however, see Ref. [31]).

It should be noted that the principal Furukawa's equations are enough complicated, and their solution requires either an iterative numerical evaluation or utilization of unphysical density of states such as the Lorentzian DOS. Note that use of the Lorentzian DOS for study of ferromagnetic phase is dangerous because it has the infinite width.

In our recent paper [32], we have offered a simple model of double exchange, which allows analytically to carry out necessary calculations (in particular, to obtain analytical expression for the band Green's function) in the dynamical mean-field approximation for the Bethe lattice with $z \to \infty$. We have defined c-operator of annihilation of a itinerant electron with spin parallel to localized spin as (see also Ref. [33])

$$c_{i\sigma} = P_{i\sigma}^{+}a_{i\sigma}, \qquad P_{i\sigma}^{+} = \frac{1}{2}(1 + \sigma S_i^z) \quad (9)$$

where $S_i^z S_i^z = 1$ and $P_{i\sigma}^{+}P_{i\sigma}^{+} = P_{i\sigma}^{+}$. One can see that: (i) c-operator (9) does not contain the factor $(1 - a_{i-\sigma}^{\dagger}a_{i-\sigma})$. In my opinion, this factor is irrelevant here because the double occupation of a site by itinerant electrons is excluded with the help of the projection operator $P_{i\sigma}^{+}$, (ii) c-operator does not take account of spin-flip processes. These processes are essential at low temperatures where thermodynamics of the system is defined, in the main, by the spin-wave excitations. However, one may neglect the spin flips for understanding of the qualitative bahaviour of physical quantities in a wide temperature range. In addition, it should be noticed that a crucial role in the electric transport near the Curie point T_{K} belongs to spatial correlation of localized spins [14,23,34,35]. This correlation is included in our simple model but it is beyond the dynamical mean-field approximation.

In the present paper, we consider the system defined by the following Hamiltonian

$$\mathcal{H} = -\frac{1}{2}\sum_i h_i S_i^z - \mu \sum_{i\sigma} c_{i\sigma}^\dagger c_{i\sigma} + \sum_{\langle ij\rangle\sigma} t_{ij} c_{i\sigma}^\dagger c_{j\sigma} - \sum_{\langle ij\rangle} J_{ij} n_{i\uparrow} n_{j\downarrow} \qquad (10)$$

where $n_{i\sigma} = c_{i\sigma}^\dagger c_{i\sigma}$, and the c-operator is defined by the relation (9). t_{ij} and J_{ij} are equal to t and J for the nearest neighbours, and $Jz = J^*$ at $z \to \infty$. For calculations of magnetization of the localized-spin subsystem and corresponding generalized paramagnetic susceptibility, we assume that the magnetic field h_i acts only on the localized spins. At the end of calculations, $h_i \to 0$.

In contrast with the reference [32], we have added the term proportional to J where $J \sim t^2/I$. This term is responsible for a possible antiferromagnetic ordering. The Hamiltonian (10) is the $t-J$ like effective Hamiltonian for the $s-f$ model with localized spins of Ising type. It can be obtained, for example, from the $t-J$ like effective Hamiltonian for the full $s-f$ model [8] with the our c-operators by the neglecting of the term with the following operator structure: $c_{i\sigma}^\dagger c_{i-\sigma} c_{j-\sigma}^\dagger c_{j\sigma}$. This term is also proportional to J but it is accountable for the spin-flip processes and its contribution to the dynamical mean-field approximation is equal to zero. In addition, note that $c_{i\sigma}^\dagger c_{i-\sigma} = 0$ for our c-operator (9). Superexchange interaction of the antiferromagnetic type is not considered.

The present paper is organized as follows. In Section 2, the exact theory of the model (10) in infinite dimensions is given. The obtained in this Section equations for the band Green's function can be solved in analytical form for the Bethe lattice ($z \to \infty$) which is considered in the following Sections. In Section 3, instability of the paramagnetic phase towards ferromagnetic and antiferromagnetic states is investigated. Properties of the ferromagnetic and the antiferromagnetic states for the Bethe lattice are studied in Sections 4 and 5. A zero-temperature phase diagram including the phase separation between ferromagnetic and antiferromagnetic states is given in Section 6. Some concluding remarks are given in the last section.

2 Simple double-exchange model in infinite dimensions

In order to obtain the exact results for the model (10) in infinite dimensions, let's present the Hamiltonian of this model in the form suitable for the direct utilizing of the results of reference [32].

As the Hartree-Fock approximation is exact in infinite dimensions for intersite interactions [26], the last term of (10) can be decoupled as

$$-\sum_{\langle ij\rangle} J_{ij}\big(\langle n_{j\downarrow}\rangle n_{i\uparrow} + \langle n_{j\uparrow}\rangle n_{i\downarrow}\big), \qquad (11)$$

and the Hamiltonian (10) can be written by the following way

$$\mathcal{H} = \mathcal{H}_0 + \mathcal{H}_{\rm int}, \qquad (12)$$

$$\mathcal{H}_0 = -\frac{1}{2}\sum_i h_i S_i^z + \sum_{i\sigma} \varepsilon_{i\sigma} c_{i\sigma}^\dagger c_{i\sigma}, \qquad (13)$$

$$\mathcal{H}_{\rm int} = \sum_{\langle ij\rangle}\sum_\sigma t_{ij} c_{i\sigma}^\dagger c_{j\sigma}, \qquad (14)$$

$$\varepsilon_{i\sigma} = -\mu - \sum_j J_{ij}\langle n_{j-\sigma}\rangle. \qquad (15)$$

$\mathcal{H}_{\rm int}$ is the perturbation operator.

Now, one can use the diagrammatic method offered in references [32,33] for a calculating of the band Green's function

$$\mathcal{G}_\sigma(i,i';\tau-\tau') = -\langle T_\tau \tilde{c}_{i\sigma}(\tau)\tilde{c}_{i'\sigma}^\dagger(\tau')\rangle \qquad (16)$$

which obeys the following equation

$$\sum_{i_1}\Big\{\big[(G^0_{s\sigma})^{ii}\big]^{-1}\delta_{ii_1} - \Sigma_{s\sigma}^{ii_1} - t_{ii_1}\Big\}\mathcal{G}_{s\sigma}^{i_1 i'} = \delta_{ii'} \qquad (17)$$

where

$$(G^0_{s\sigma})^{ii'} = \frac{\delta_{ii'}}{{\rm i}\omega_s - \varepsilon_{i\sigma}}, \qquad (18)$$

$$\mathcal{G}_{s\sigma}^{ii'} \equiv \mathcal{G}_\sigma(i,i';{\rm i}\omega_s), \quad \Sigma_{s\sigma}^{ii'} \equiv \Sigma_\sigma(i,i';{\rm i}\omega_s) \qquad (19)$$

and $\omega_s = (2s+1)\pi T$.

The self-energy part is a local function in infinite dimensions [25,26]

$$\Sigma_{s\sigma}^{ii'} = \Sigma_{s\sigma}^{ii}\delta_{ii'} \qquad (20)$$

and, as a result, we obtain the following expression for $\Sigma_{s\sigma}^{ii}$ [32]

$$\Sigma_{s\sigma}^{ii} = -\frac{\frac{1}{2}(1-\sigma m_i^f)}{\mathcal{G}_{s\sigma}^{ii}}\,. \qquad (21)$$

where $m_i^f = \langle S_i^z\rangle$.

This result is similar to the expression for the self-energy part Σ_s^{ii} in the spinless Falicov-Kimball model with large interaction in infinite dimensions [36].

The equations (17), (20) and (21) are the equations for $\mathcal{G}_{s\sigma}^{ii}$, the diagonal part of $\mathcal{G}_{s\sigma}^{ii'}$, and $\Sigma_{s\sigma}^{ii}$. In the following Sections we shall show that these equations are exactly solved in analytical form in the case of Bethe lattice with $z \to \infty$ both for ferromagnetic and antiferromagnetic phase.

The equation for m_i^f can be also obtained with the help of the diagrammatic technique for the c-operators. Using the results of reference [32], we have

$$m_i^f = \tanh\frac{1}{2}\lambda_i, \qquad \lambda_i = \lambda_i^0 + \eta_i \qquad (22)$$

where

$$\lambda_i^0 = y_i^f + \ln\frac{1+\exp(\beta\mu_{\rm r}-y_i^s)}{1+\exp(\beta\mu_{\rm r}+y_i^s)}, \tag{23}$$

$$y_i^f = \beta h_i, \qquad y_i^s = \frac{1}{2}\beta\sum_j J_{ij}m_j^s, \tag{24}$$

$$\eta_i = \sum_s\left\{\ln\frac{(1+m_i^f)(G_{s\uparrow}^0)^{ii}}{2\mathcal{G}_{s\uparrow}^{ii}} - \ln\frac{(1-m_i^f)(G_{s\downarrow}^0)^{ii}}{2\mathcal{G}_{s\downarrow}^{ii}}\right\}, \tag{25}$$

$\beta = 1/T$, $m_i^s = \langle n_{i\uparrow}\rangle - \langle n_{i\downarrow}\rangle$, $\mu_{\rm r} = \mu + J^*n/2$ is the renormalized chemical potential and $n = \langle n_{i\uparrow}\rangle + \langle n_{i\downarrow}\rangle$ is the total concentration of itinerant electrons; we assume that the subsystem of itinerant electrons has a homogeneous charge distribution.

It is necessary to note that the average

$$\langle S_i^z\rangle_0 = \frac{{\rm Tr}\left({\rm e}^{-\beta\mathcal{H}_0}S_i^z\right)}{{\rm Tr}\,{\rm e}^{-\beta\mathcal{H}_0}} \tag{26}$$

is required to calculate m_i^f. It is determined with taking into account that a site has four states: two states without itinerant electrons and two states in which spin of a single band electron is parallel to localized spin. Therefore,

$$\langle S_i^z\rangle_0 = \frac{\sinh\left(\frac{1}{2}y_i^f\right) + {\rm e}^{\beta\mu_{\rm r}}\sinh\left(\frac{1}{2}y_i^f - y_i^s\right)}{\cosh\left(\frac{1}{2}y_i^f\right) + {\rm e}^{\beta\mu_{\rm r}}\cosh\left(\frac{1}{2}y_i^f - y_i^s\right)} = \tanh\frac{1}{2}\lambda_i^0. \tag{27}$$

From equation (22), one can obtain the expression for the generalized paramagnetic susceptibility as a derivative of m_i^f with respect to $h_{i'}$:

$$\chi(i,i') = \left.\frac{{\rm d}m_i^f}{{\rm d}h_{i'}}\right|_{m_i^f,m_i^s,h_{i'}\to 0}. \tag{28}$$

For this purpose, it is convenient to use the method of reference [37], and we have the following expression for the Fourier transform $\chi(\mathbf{q})$ of $\chi(i,i')$:

$$\chi(\mathbf{q}) = \frac{\frac{1}{2}}{T - \frac{1}{2}\left[Y(\mathbf{q}) - V^2(\mathbf{q})J_{\rm eff}(\mathbf{q})\right]} \tag{29}$$

where

$$J_{\rm eff}(\mathbf{q}) = \frac{J(\mathbf{q})}{1 - J(\mathbf{q})Z(\mathbf{q})}, \tag{30}$$

$$V(\mathbf{q}) = T\sum_s \frac{\mathcal{G}_s\chi_s^0(\mathbf{q})}{\mathcal{G}_s^2 - \frac{1}{2}\chi_s^0(\mathbf{q})}, \tag{31}$$

$$Y(\mathbf{q}) = 2T\sum_s \frac{\mathcal{G}_s^2 - \chi_s^0(\mathbf{q})}{\mathcal{G}_s^2 - \frac{1}{2}\chi_s^0(\mathbf{q})}, \tag{32}$$

$$Z(\mathbf{q}) = T\sum_s \frac{\mathcal{G}_s^2\chi_s^0(\mathbf{q})}{\mathcal{G}_s^2 - \frac{1}{2}\chi_s^0(\mathbf{q})}, \tag{33}$$

$$\chi_s^0(\mathbf{q}) = \frac{1}{N}\sum_{\mathbf{k}}\mathcal{G}_s(\mathbf{k})\mathcal{G}_s(\mathbf{k}+\mathbf{q}) \tag{34}$$

and $\mathcal{G}_s$ is the band Green's function $\mathcal{G}_{s\sigma}^{ii}$ taken at $h_i = m_i^f = m_i^s = 0$.

We shall be in need of the internal energy. We have

$$E(T) = \sum_{\langle ij\rangle\sigma} t_{ij}\langle c_{i\sigma}^\dagger c_{j\sigma}\rangle - \sum_{\langle ij\rangle} J_{ij}\langle n_{i\uparrow}\rangle\langle n_{j\downarrow}\rangle$$
$$= T\sum_s\sum_{i\sigma}\left\{-\frac{1}{2}\sigma m_i^f + \left({\rm i}\omega_s + \mu_{\rm r} - \frac{1}{2}\sigma\sum_j J_{ij}m_j^s\right)\mathcal{G}_{s\sigma}^{ii}\right\}$$
$$-\frac{1}{4}J^*Nn^2 + \frac{1}{4}\sum_{\langle ij\rangle} J_{ij}m_i^s m_j^s. \tag{35}$$

3 Instability of the paramagnetic phase

In this and the following Sections, we shall consider the Bethe lattice with $z\to\infty$ for which density of state has the form

$$\rho_0(\varepsilon) = \frac{4}{\pi W}\sqrt{1-(2\varepsilon/W)^2}, \quad -\frac{1}{2}W < \varepsilon < \frac{1}{2}W \tag{36}$$

where W is the bare bandwidth.

In the case of the Bethe lattice, the system of the equations (17) and (21) for $\mathcal{G}_{s\sigma}^{ii}$ and $\Sigma_{s\sigma}^{ii}$ is exactly solved in analytical form, and we have the following expression for the function $\mathcal{G}_{s\sigma}^{ii} \equiv \mathcal{G}_s$:

$$\mathcal{G}_s = \frac{8}{W^2}\left\{\Omega_s - \sqrt{\Omega_s^2 - W^2/8}\right\}, \tag{37}$$

$\Omega_s = {\rm i}\omega_s + \mu_{\rm r}$, for the paramagnetic phase ($m_i^f = m_i^s = h_i = 0$).

It is seen from (37) that the correlation bandwidth is equal to $W/\sqrt{2}$ in the paramagnetic state. This value coincides with the fermion bandwidth obtained in reference [23] in infinite temperature limit.

We shall consider the susceptibility (29) in two cases: $\mathbf{q} = \mathbf{0}$ (uniform susceptibility) and $\mathbf{q} = \mathbf{Q} = (\pi,\pi,\ldots\pi)$ (staggered susceptibility).

In the case of $\mathbf{q} = \mathbf{0}$, we have $J(\mathbf{0}) = J^*$,

$$\chi_s^0(\mathbf{0}) = \frac{\mathcal{G}_s}{\Omega_s - \Sigma_s - a^2\mathcal{G}_s}, \tag{38}$$

$a^2 = W^2/8$, and

$$\chi(\mathbf{0}) = \frac{\frac{1}{2}}{T - \frac{1}{2}\left[Y(\mathbf{0}) - V^2(\mathbf{0})J_{\rm eff}(\mathbf{0})\right]}, \tag{39}$$

$$J_{\rm eff}(\mathbf{0}) = \frac{J^*}{1 + J^*Y(\mathbf{0})/a^2}, \tag{40}$$

$$V(\mathbf{0}) = \frac{1}{\pi}\int_0^\pi {\rm d}t f(a\cos t), \tag{41}$$

$$Y(\mathbf{0}) = -\frac{a}{\pi}\int_0^\pi {\rm d}t\cos t f(a\cos t)$$
$$= -a^2\frac{1}{\pi}\int_0^\pi {\rm d}t\sin^2 t\frac{{\rm d}f(a\cos t)}{{\rm d}(a\cos t)}, \tag{42}$$

$f(x) = [\exp\beta(x-\mu_{\rm r})+1]^{-1}$ is the Fermi-Dirac function with the renormalized chemical potential $\mu_{\rm r}$.

In the case of $\mathbf{q}=\mathbf{Q}$, we have $J(\mathbf{Q}) = -J^*$,

$$\chi_s^0(\mathbf{Q}) = \frac{\mathcal{G}_s}{\Omega_s - \Sigma_s} \tag{43}$$

and

$$\chi(\mathbf{Q}) = \frac{\frac{1}{2}}{T - \frac{1}{2}\big[Y(\mathbf{Q}) - f^2(0)J_{\rm eff}(\mathbf{Q})\big]}, \tag{44}$$

$$J_{\rm eff}(\mathbf{Q}) = -\frac{J^*}{1 + J^* Y(\mathbf{Q})/a^2}, \tag{45}$$

$$Y(\mathbf{Q}) = \frac{a}{\pi}\int\limits_0^\pi {\rm d}t \frac{\sin^2 t}{\cos t} f(a\cos t). \tag{46}$$

The expressions (39) and (44) must be used jointly with the following equation

$$\frac{1}{2}n = T\sum_s \mathcal{G}_s = \frac{1}{\pi}\int\limits_0^\pi {\rm d}t \sin^2 t f(a\cos t) \tag{47}$$

for the chemical potential μ.

It is easy to see that the high-temperature expansion of $\chi(\mathbf{0})$ taken at $J^*=0$ contains only odd powers of $1/T$. Similar situation was marked long ago in reference [2] where double exchange was considered in the scope of a two-atom system. The high-temperature expansion of the uniform susceptibility in reference [2] does not include the term proportional to $1/T^2$, which is what served the authors of reference [2] as a reason for concluding that the susceptibility obeys Curie law at high temperatures, and that it has inverse curvature in comparison with Heisenberg one at low temperatures. Our dynamical mean-field calculations for the Bethe lattice confirm this qualitative conclusion (see also Ref. [32]).

The exact high-temperature expansion (EHTE) of the uniform susceptibility for the z-coordinated Bethe lattices and s.c. lattice shows that, although the series for $\chi(\mathbf{0})$ contains only odd powers of $1/T$ for these lattices, $\chi(\mathbf{0})$ has Curie-Weiss behaviour for all electron concentrations [38]. (Curie-Weiss behaviour of $\chi(\mathbf{0})$ was also found in reference [39] for 1D and 2D systems). EHTE method had given good results for the Heisenberg and the Ising models for which enough terms in series for $\chi(\mathbf{0})$ were calculated. Unfortunately, the authors of reference [38] have not informed about the amount of calculated terms but it seems that a discussion of the critical behaviour of DE system requires a more advanced calculation.

Similar temperature behaviour is also observed for the inverse staggered susceptibility ($J^* \neq 0$) at $n<1$. However, $\chi(\mathbf{Q})$ exactly obeys Curie-Weiss law at $n=1$. In this case, the model (10) has the form

$$\mathcal{H} = \frac{1}{4}\sum_{\langle ij\rangle} J_{ij} S_i^z S_j^z, \tag{48}$$

and Néel temperature $T_{\rm N}$ is equal to $J^*/2$.

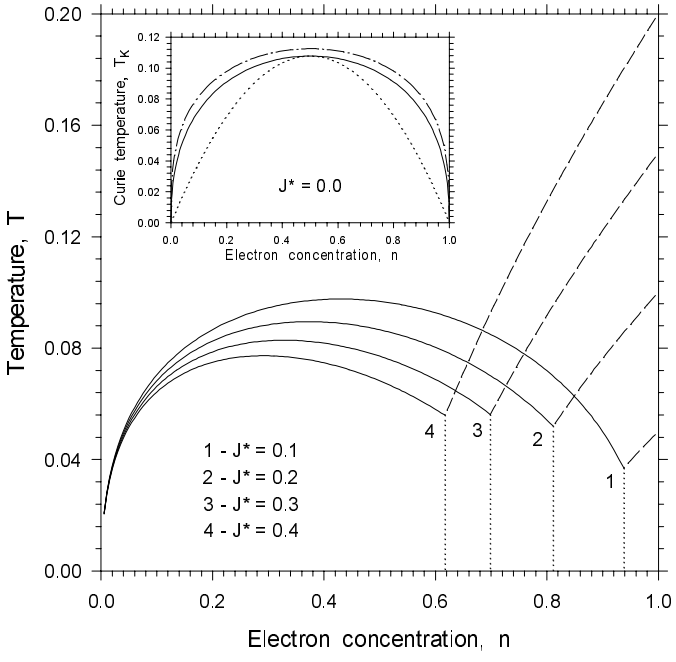

Fig. 1. Electron-concentration dependences of Curie temperature (solid curve) and Néel temperature (dashed curve) for different values of J^*. The inset shows Curie temperature as a function of electron concentration at $J^*=0$ (see the text).

Investigation of the critical behaviour of the staggered susceptibility for any n requires also a more accurate analysis.

Electron-concentration dependences of the transition temperatures $T_{\rm K}$ and $T_{\rm N}$ are shown in Figure 1. We observe the expected suppression of $T_{\rm K}$ and the increasing of $T_{\rm N}$ due to J-interaction. Problem of phase state below the intersection point of $T_{\rm K}$ and $T_{\rm N}$ curves at given J^* requires additional investigation. In Section 6, we shall show that the system (10) is unstable towards the phase separation between ferromagnetic and antiferromagnetic states when $T=0$.

The inset to Figure 1 shows dependence of $T_{\rm K}$ on the electron concentration n (solid curve) at $J^*=0$. Dotted curve is the scaled plot of $n(1-n)$. Dashed-dotted curve presents $T_{\rm K}$ calculated from the following expression

$$T_{\rm K} = \frac{1}{2}a\frac{1}{\pi}\sqrt{1-(\varepsilon_{\rm F}/a)^2} = \frac{W^2}{16}\rho(\varepsilon_{\rm F}) \tag{49}$$

where $\rho(\varepsilon)$ is the density of states of the correlation band. The formula (49) can be obtained from $Y(\mathbf{0})$ (see (42)) taken at $T=0$. As $Y(\mathbf{0})/a^2$ has the form of the polarization operator taken at the zero momentum, we think that the expression (49) is suitable in the dynamical mean-field approximation for any crystal.

The maximum value of $2T_{\rm K}/W$ is equal to 0.108 ($n=0.5$). When $W\sim 1$ eV (this estimate of W is used by Furukawa [30]), $T_{\rm K}\sim 630$ K. However, taking into account that: (i) $T_{\rm K}$ is measured in materials with non-zero J^* (apparently, $2J^*/W\sim 0.1$) or (and) non-zero superexchange interaction and at $0.6<n<0.8$, (ii) mean-field

theory always overestimates the value of transition temperature, (iii) $T_{\rm K}$ is essentially decreased when the coordination number z is decreased (see Ref. [38]), one can conclude that double exchange alone can in principle explain the values of $T_{\rm K}$ at least for the high-$T_{\rm K}$ manganese oxides (*e.g.* LSMO where $T_{\rm K} \simeq 380$ K). This consequence agrees to the Furukawa's conclusion about capability of DE to explain the value of $T_{\rm K}$ in LSMO. In connection with it, see references [10,11,15,17,18,22,29,38–41] where were obtained still smaller values of $T_{\rm K}$.

4 Ferromagnetic phase

In this case,

$$m_i^s = m^s, \qquad m_i^f = m^f, \tag{50}$$

$$\mathcal{G}_{s\sigma}^{ii} \equiv \mathcal{G}_s = \frac{8}{W^2}\Big\{\Omega_s - \sigma\nu - \sqrt{(\Omega_s - \sigma\nu)^2 - a_\sigma^2}\Big\}, \tag{51}$$

and we have the following equations

$$m^f = \tanh\frac{1}{2}\lambda_{\rm F}, \tag{52}$$

$$\lambda_{\rm F} = \frac{1}{\pi}\int\limits_0^\pi {\rm d}t \ln\frac{1+\exp\beta(\mu_r - \nu - a_\uparrow\cos t)}{1+\exp\beta(\mu_r + \nu - a_\downarrow\cos t)}, \tag{53}$$

$$n = \sum_\sigma (1+\sigma m^f)\frac{1}{\pi}\int\limits_0^\pi {\rm d}t \sin^2 t f(a_\sigma\cos t + \sigma\nu), \tag{54}$$

$$m^s = nm^f + [1-(m^f)^2] \times \sum_\sigma \sigma\frac{1}{\pi}\int\limits_0^\pi {\rm d}t \sin^2 t f(a_\sigma\cos t + \sigma\nu), \tag{55}$$

$$a_\sigma^2 = \frac{1}{8}W^2(1+\sigma m^f), \qquad \nu = \frac{1}{2}J^* m^s \tag{56}$$

describing the ferromagnetic phase (the formula (3.22) in Ref. [32] has a numerical mistake — the factor 1/2 before η is lacking). The equations (52), (54) and (55) determine m^f, m^s and μ at given n and J^*.

The band picture is defined by the quantity a_σ which is the halfwidth of the correlation band for σ-electrons. When m^f is decreased, $\uparrow$-subband is narrowed and $\downarrow$-subband is extended. $a_\uparrow = a_\downarrow = a = W/2\sqrt{2}$ in the paramagnetic case.

Correlation change of subbandwidths is responsible for many properties of ordered phases. In particular, it naturally accounts for negative temperature shift of the chemical potential in the ferromagnetic state (see also Ref. [30]). It turns out that approximately

$$\mu(T) = \mu(T_{\rm K}) + \alpha(n)(T_{\rm K} - T), \tag{57}$$

$\alpha(n) > 0$, in a wide temperature range below $T_{\rm K}$ at $J^* = 0$. In the paramagnetic phase,

$$\mu(T) = \mu(T_{\rm K}) + \beta(n)(T - T_{\rm K}), \tag{58}$$

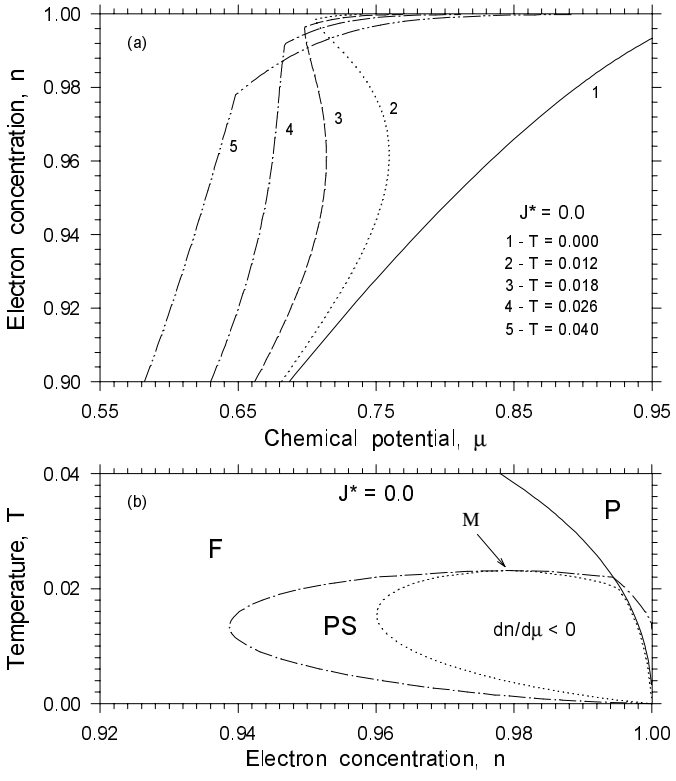

Fig. 2. (a) The electron concentration as a function of the chemical potential for different temperatures, (b) temperature phase diagram of DE system for $J^* = 0$: solid curve is the Curie-temperature curve (see the inset to the Fig. 1), dotted curve determines the region with the negative compressibility and dashed-dotted curve determine the phase separation (PS) region. F(P) denotes ferromagnetic (paramagnetic) state. The point M is the point in which two PS-transition curves are converged.

where $\beta(n) > 0$. Thus, ${\rm d}\mu/{\rm d}T$ changes a sign at $T = T_{\rm K}$. If we accept that the thermopower is propotional to ${\rm d}\mu/{\rm d}T$ [17], it roughly have a jump at $T = T_{\rm K}$ in our approach. When $T < T_{\rm K}$, the thermopower anomalously has the negative sign. In the paramagnetic phase, the temperature dependence of the bandwidth vanishes, and the usual sign is restored.

Let us consider μ-dependence of the electron concentration n, which is shown in Figure 2a for $J^* = 0$ and different T. Break in a curve occurs at some critical value $n_{\rm c}$ of n such that the ferromagnetism arises at $n < n_{\rm c}$ for given T. For the curve 1 ($T = 0$) $n_{\rm c} = 1$. It is seen from Figure 2a that there are temperatures for which the compressibility ${\rm d}n/{\rm d}\mu$ has the negative sign. (Influence of critical long-wave charge fluctuations on resistivity in DE system near ${\rm d}n/{\rm d}\mu = \infty$ is discussed in Ref. [13]). It means that the system is unstable towards phase separation (PS) at these temperatures. The (n,T)-region with the negative ${\rm d}n/{\rm d}\mu$ is shown in Figure 2b where the results of Maxwell construction are also presented. One can distinguish two features of PS at $J^* = 0$: (i) the point M, in which two PS-transition curves (they determine

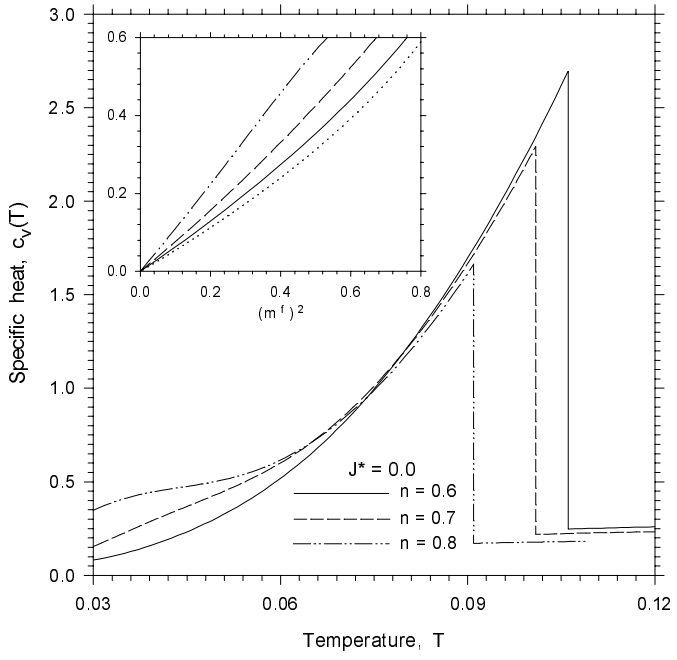

Fig. 3. Specific heat as a function of temperature for $J^* = 0$ and different values of n. The inset shows dependence of $1 - c_{\rm v}(T)/c_{\rm v}(T_{\rm K})$ on $(m^f)^2$ at the same values of n (the same types of curves) for DE system and for the Heisenberg system (dotted curve) in the mean-field approximation.

concentrations of electron-poor and electron-rich spatial regions for given T) are converged, is inside of the ferromagnetic phase region, (ii) the absence of PS at $T = 0$. The last feature is marked in reference [17] where PS was investigated in the frame of a static mean-field approximation. In contrast with our results, the M-point in the phase diagram of reference [17] is inside of the paramagnetic region. Thus, PS of this type is temperature effect of the DE system with $J^* = 0$. The system separates into electron-rich regions with the paramagnetic state and electron-poor regions with the ferromagnetic state at nonzero temperatures. In very narrow temperature range below the M-point, the system separates into electron-poor and electron-rich regions with the ferromagnetic state.

Figure 3 shows temperature behaviour of the specific heat

$$c_{\rm v}(T) = \frac{{\rm d}E_{\rm F}(T)}{{\rm d}T} \tag{59}$$

for $J^* = 0$ and different values of n. The internal energy $E_{\rm F}(T)$ is calculated for the ferromagnetic phase from (35), and

$$\frac{E_{\rm F}(T)}{N} = -\frac{1}{4}J^*\left[n^2 - (m^s)^2\right] + W\sum_\sigma\left(\frac{1+\sigma m^f}{2}\right)^{3/2} \times \frac{1}{\pi}\int\limits_0^\pi {\rm d}t \sin^2 t \cos t f(a_\sigma \cos t + \sigma\nu). \tag{60}$$

It is interesting to compare the results in Figure 3 with the behaviour of $c_{\rm v}$ for the Heisenberg model in the mean-field approximation. The inset to Figure 3 shows dependence of $1 - c_{\rm v}(T)/c_{\rm v}(T_{\rm K})$ on $(m^f)^2$ for the same value of n as in Figure 3 (the same type of curves) and for the Heisenberg system (dotted curve). We observe a similar behaviour of dotted and solid ($n = 0.6$) curves in a wide temperature range below $T_{\rm K}$. Temperature range of this similarity are decreased for $n = 0.7$ and $n = 0.8$. In any case, we approximately have

$$c_{\rm v}(T) = c_{\rm v}(T_{\rm K}) - \gamma(n)(m^f)^2, \quad \gamma(n) > 0, \text{ at } (T_{\rm K} - T)/T_{\rm K} \ll 1. \tag{61}$$

5 Antiferromagnetic phase

In the case of the antiferromagnet with two sublattices A and B, we have

$$m_i^f = q_i m^f, \qquad m_i^s = q_i m^s, \tag{62}$$

$$q_i = \begin{cases} +1, & i \in A \\ -1, & i \in B \end{cases}, \tag{63}$$

and the equations for $\mathcal{G}_{s\sigma}^{ii}$ and $\Sigma_{s\sigma}^{ii}$ can be also solved in analytical form for the Bethe lattice ($z \to \infty$). As a result, we obtain

$$\mathcal{G}_{s\sigma}^{ii} = \mathcal{G}_s^{(1)} + \sigma q_i \mathcal{G}_s^{(2)}, \tag{64}$$

$$\mathcal{G}_s^{(1)} = -\frac{\frac{1}{2}m^f\nu}{\Omega_s^2 - \nu^2} + \frac{8}{W^2}\Omega_s\left\{1 - \frac{1}{\Omega_s^2 - \nu^2}\sqrt{(\Omega_s^2 - \omega_1^2)(\Omega_s^2 - \omega_2^2)}\right\}, \tag{65}$$

$$\mathcal{G}_s^{(2)} = \frac{\frac{1}{2}m^f\Omega_s}{\Omega_s^2 - \nu^2} - \frac{8}{W^2}\nu\left\{1 - \frac{1}{\Omega_s^2 - \nu^2}\sqrt{(\Omega_s^2 - \omega_1^2)(\Omega_s^2 - \omega_2^2)}\right\}. \tag{66}$$

Here,

$$\omega_1^2 = \nu^2 + \frac{W^2}{8}\alpha_1^2, \qquad \omega_2^2 = \nu^2 + \frac{W^2}{8}\alpha_2^2,$$

$$\alpha_1^2 = \frac{1}{2} - \frac{1}{2}\sqrt{1 - (m^f)^2}, \quad \alpha_2^2 = \frac{1}{2} + \frac{1}{2}\sqrt{1 - (m^f)^2}. \tag{67}$$

With the help of equations (65) and (66), one can obtain the following equations

$$m^f = \tanh\frac{1}{2}\lambda_A, \tag{68}$$

$$\lambda_{\rm A} = 2\ln\Big(1+{\rm e}^{\beta(\mu_{\rm r}+\nu)}\Big) - \alpha_1\alpha_2\frac{2}{\pi}\int\limits_0^{\pi/2}\frac{{\rm d}t}{\alpha_1^2\sin^2 t+\alpha_2^2\cos^2 t} \times\Big\{\ln\Big(1+{\rm e}^{\beta[\mu_{\rm r}+E(t)]}\Big)+\ln\Big(1+{\rm e}^{\beta[\mu_{\rm r}-E(t)]}\Big)\Big\}, \tag{69}$$

$$m^s = m^f f(-\nu) - [1-(m^f)^2]\nu \times\frac{2}{\pi}\int\limits_0^{\pi/2}\frac{{\rm d}t\sin^2 t\cos^2 t}{\alpha_1^2\sin^2 t+\alpha_2^2\cos^2 t}\frac{f[E(t)]-f[-E(t)]}{E(t)}, \tag{70}$$

$$n = m^f f(-\nu) + [1-(m^f)^2] \times\frac{2}{\pi}\int\limits_0^{\pi/2}\frac{{\rm d}t\sin^2 t\cos^2 t}{\alpha_1^2\sin^2 t+\alpha_2^2\cos^2 t}\big(f[E(t)]+f[-E(t)]\big), \tag{71}$$

$$E(t) = \sqrt{\frac{1}{8}W^2\big(\alpha_1^2\sin^2 t+\alpha_2^2\cos^2 t\big)+\nu^2} \tag{72}$$

describing the antiferromagnetic state of the Bethe lattice in the dynamical mean-field approximation.

The equations (68), (70) and (71) determine m^f, m^s and μ for given n and J^*.

We also give the expression for the internal energy of the antiferromagnetic state:

$$E_{\rm A}(T)/N = -\frac{1}{4}J^*[n^2+(m^f)^2]+\frac{1}{4}W^2[1-(m^f)^2] \times\frac{1}{\pi}\int\limits_0^{\pi/2}{\rm d}t\sin^2 t\cos^2 t\frac{f[E(t)]-f[-E(t)]}{E(t)}. \tag{73}$$

It is seen from (72) that the band picture is defined by two subbands. The boundaries of these subbands are

$$-\sqrt{\frac{1}{8}W^2\alpha_2^2+\nu^2}, \qquad -\sqrt{\frac{1}{8}W^2\alpha_1^2+\nu^2} \tag{74}$$

for the bottom subband and

$$\sqrt{\frac{1}{8}W^2\alpha_1^2+\nu^2}, \qquad \sqrt{\frac{1}{8}W^2\alpha_2^2+\nu^2} \tag{75}$$

for the top subband. The subbands are mixed into one band when $m^f = m^s = 0$.

Assuming that the ferromagnetic alignment is absent, let us discuss a possible phase separation between the antiferromagnetic and the paramagnetic states. Investigation of the compressibility ${\rm d}n/{\rm d}\mu$ with the help of the equations (68), (70) and (71) shows that our DE system is unstable with regard to PS only for $J^* > J_{\rm c}^* \simeq 0.318$. It turns out that PS occurs inside of the antiferromagnetic phase for J^* near $J_{\rm c}^*$. In contrast with the ferromagnetic case, the PS state has a maximum concentration range at $T = 0$. When T is increased, the PS is strongly suppressed. For example, the compressibility is negative at $0.882 < n < 0.990$ ($T = 0$) in the case of $J^* = 0.34$ and at $0.749 < n < 0.996$ ($T = 0$) for $J^* = 0.4$. These concentration ranges correspond to the antiferromagnetic state of DE system at $T = 0$ When T is increased, the concentration range of negative compressibility is decreased, and PS vanishes at the phase point ($n = 0.936, T = 0.0023$) for $J^* = 0.34$ and at the phase point ($n = 0.867, T = 0.0114$) for $J^* = 0.4$. These critical phase points also belong to the antiferromagnetic phase region.

When $J^* > 0.4$, PS between antiferromagnetic and paramagnetic states is possible. However, these values of J^* are very large (see Fig. 1), and we do not discuss this case.

Thus, if we do not include ferromagnetic state, phase separation of any type is lacking for $J^* < J_{\rm c}^*$. Taking into account that the experimental values of J^* for the manganese oxides do not exceed $J_{\rm c}^*$, one can conclude that PS connected with antiferromagnetic and paramagnetic states is not realized in real materials from the standpoint of our approach.

6 Phase diagram at T = 0

Our phase diagram of the model (10) includes two phase states (ferromagnetic and antiferromagnetic) at $T = 0$. Paramagnetic phase is the high-temperature state, and we do not consider a phase with incommensurate correlation and a canted phase.

When instability of the paramagnetic state towards two ordered phases was discussed (Sect. 3), we have marked that there is a phase region in which regions of instability of the paramagnetic phase with regard to antiferromagnetic and ferromagnetic states are overlapped. This common phase region lies below the point of intersection of the antiferromagnetic and the ferromagnetic transition curves for given J^* (see Fig. 1). When $T = 0$, the discussed region has a maximum spread over the electron concentration. In Figure 4b, it lies between dashed and dashed-dotted curves which are the second-order transition curves:

$$J_{\rm F}^* = \frac{Y(\mathbf{0})}{V^2(\mathbf{0})-Y^2(\mathbf{0})/a^2} \tag{76}$$

for the ferromagnetic transition and

$$J_{\rm A}^* = -\frac{Y(\mathbf{Q})}{Y^2(\mathbf{Q})/a^2+f^2(0)} \tag{77}$$

for the antiferromagnetic transition. All the quantities in (76) and (77) are taken at $T = 0$.

Question about the choice of the state, which is realized in a given phase point at $T = 0$, is solved by the comparing of the ground-state energies. The energies of ferromagnetic and the antiferromagnetic ground states can be

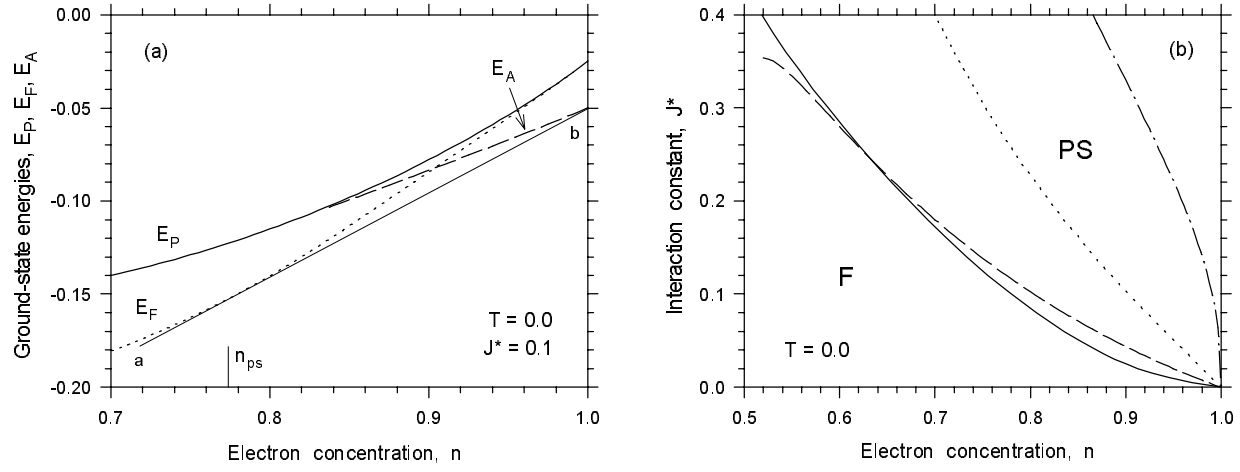

Fig. 4. (a) Ground-state energies $E_{\rm P}$, $E_{\rm F}$ and $E_{\rm A}$ as functions of n. The straight line ab realizes Maxwell construction. n_{ps} is the concentration of electron-poor spartial domains. (b) Phase diagram at $T = 0$. Dashed (dashed-dotted) curve is curve of the antiferromagnetic (ferromagnetic) second-order transition. $E_{\rm F} = E_{\rm A}$ on dotted curve. The PS region lies between solid curve and the axis $n = 1$. The pure ferromagnetic state is on the left from solid line and the pure antiferromagnetic state is on the axis $n = 1$.

obtained from (60) and (73) with the corresponding equations for m^f, m^s and μ taken at $T = 0$. The expressions for $E_{\rm F}(T = 0) \equiv E_{\rm F}$ and $E_{\rm A}(T = 0) \equiv E_{\rm A}$ are coordinated with the corresponding equations for m^f, m^s and μ so that the total derivative of $E_{\rm F}$ and $E_{\rm A}$ with respect to n is equal to μ.

Figure 4a shows the energies $E_{\rm F}$, $E_{\rm A}$ and $E_{\rm P}$ ($E_{\rm P}$ is the energy of paramagnetic ground state) as functions of n for $J^* = 0.1$. It is seen that $E_{\rm F} < E_{\rm P}$ and $E_{\rm A} < E_{\rm P}$. It is also seen that there is a value of $n = n^*$ at which $E_{\rm A} = E_{\rm F}$. Therefore, the ferromagnetic state is realized at $n < n^*$ where $E_{\rm F} < E_{\rm A}$, and $E_{\rm A} < E_{\rm F}$ when $n > n^*$. Here, the antiferromagnetic state is the ground state.

Thus, the ground-state energy of DE system as a function of n is presented by $E_{\rm F}$ when $0 \le n \le n^*$ and $E_{\rm A}$ when $n^* \le n \le 1$. However, this function is not convex function (see Fig. 4a). The Maxwell construction (the straight line ab) determines two values of n: $n = n_{ps}$ and $n = 1$, and DE system separates into electron-poor ($n = n_{ps}$) domains with ferromagnetic state and electron-rich ($n = 1$) domains with antiferromagnetic state.

Figure 4b shows the PS phase region limited by the solid curve and the axis $n = 1$. The pure antiferromagnetic state takes place only at $n = 1$. On the dotted curve, $E_{\rm F} = E_{\rm A}$.

It should be noted that PS of this type was first discussed by Visscher [42] for the Hubbard model and Nagaev for the $s - f$ model [43] in the strongly correlated regime. Nagaev has shown that PS state is energetically preferable in contrast with a canted phase (see also Refs. [30,44]).

Taking into account the absence of the phase separations connected with antiferromagnetic and paramagnetic states for $J^* < J^*_{\rm c}$ at any temperatures, one can roughly represent a temperature phase diagram for a given $J^* < J^*_{\rm c}$ with the help of Figures 1 and 4b. Such a temperature phase diagram must consist of the corresponding phase-transition curves (antiferromagnetic and ferromagnetic) from Figure 1 and two curves defining a PS region between antiferromagnetic and ferromagnetic states. One of them connects the point of intersection of antiferromagnetic and ferromagnetic transition curves with a point on the axis $n = 1$ at a non-zero temperature. The other curve connects the same point of intersection of transition curves with a point on the axis $T = 0$. Coordinate of the last point can be obtained from Figure 4b for the corresponding value of J^*. High-temperature phase separation between electron-poor paramagnetic region and electron-rich antiferromagnetic region does not occur at $J^* < J^*_{\rm c}$.

Recently, temperature phase diagram was investigated within the $s - f$ model with classical localized spins for Bethe lattice [10,11,30]. Starting from a random spin configuration, the dynamical mean-field equations [29,30] for this model was solved iteratively in the case of $2I/W = 4.0$. The phase diagram obtained in references [10,11,30] is coincided in common features with our consideration. But in contrast with our conclusion about the absence of PS between antiferromagnetic and paramagnetic states at $J^* < J^*_{\rm c}$, it contains such PS region so that the pure antiferromagnetic state is realized only on the axis $n = 1$ at any temperatures. Unfortunately, the authors of references [10,11,30] did not investigate PS of this type as a function of W/I but it seems that there is a critical value of W/I below of which this PS is lacking.

In connection with it, it is interesting to mark that the mathematical structure of the model (10) is similar to the one of the $t - J$ model. (See, for example, Ref. [45] about the equivalence of the $s - f$ and Hubbard models in the strongly correlated regime). Investigation of the PS between antiferromagnetic and paramagnetic states for this model shows that majority of the authors concludes that PS of this type is impossible for small values of J.

7 Concluding remarks

In the present paper, we have offered a simple model of DE system. This model takes account of the main physical feature of DE which is the parallelism of itinerant electron spin and localized spin in the same site.

Mathematical simplicity of the model allows to carry out the correct investigation of DE in the frame of the dynamical mean-field approximation and to obtain the equations describing the main ordered phases in analytical form. Using these equations, we have investigated the instability conditions of the paramagnetic phase towards the ferromagnetic and antiferromagnetic states, some properties of the ferromagnetic phase (such as the negative temperature shift of the chemical potential, the temperature dependence of the thermopower and the specific heat near the critical point, the temperature PS between ferromagnetic and paramagnetic phases) and the antiferromagnetic phase. Phase diagram including a PS between antiferromagnetic and ferromagnetic states was built at $T = 0$. It was shown that PS connected with the paramagnetic and the antiferromagnetic states is lacking for $J^* < J_c^* \simeq 0.318$ for any temperatures. It seems that these values of J^* are relevant for the real materials, and PS between antiferromagnetic and ferromagnetic states is the main type of PS in the manganese oxides.

An important aspect of study of DE system is discussion of possible non-Heisenberg behaviour of the physical quantities in dependence on the electron concentration. This peculiarity was still marked by Anderson and Hasegawa [2] in temperature behaviour of the uniform susceptibility.

Summarizing our results, one can say that, in the main, our DE system is similar to the Heisenberg ferromagnet with non-regular localized spins, and it can reveal a non-Heisenberg temperature behaviour of magnetic quantities. (It should be spoken about the Ising-type behaviour because the model (10) ignores transverse spin fluctuations.) In connection with it, it is interesting to investigate the critical behaviour of DE system with the help of the exact high-temperature expansion. It seems that a simplicity of our model allows correctly to carry out this calculation.

Of course, the model (10) has a limited practical interest and it can be used for real materials with a strong magnetic anisotropy along the z-direction. However, it seems that our model can be useful for general understanding of physical properties of DE systems in a wide temperature range.

This work is supported by Russian Fond of Fundamental Research, project 99-02-16279.

References

1. C. Zener, Phys. Rev. **82**, 403 (1951).
2. P.W. Anderson, H. Hasegawa, Phys. Rev. **100**, 675 (1955).
3. P.-G. de Gennes, Phys. Rev. **118**, 141 (1960).
4. K. Kubo, N. Ohata, J. Phys. Soc. Jpn **33**, 21 (1972).
5. G.H. Jonker, J.H. van Santen, Physica **16**, 337, 599 (1950).
6. A.P. Ramirez, J. Phys. Cond. Matter **9**, 8171 (1997).
7. S.V. Vonsovskii, JETP **16**, 981 (1946).
8. S.Q. Shen, Z.D. Wang, Phys. Rev. B **58**, R8877 (1998).
9. E. Müller-Hartmann, E. Dagotto, Phys. Rev. B **54**, R6819 (1996).
10. S.Yunoki, J. Hu, A.L. Malvezzi, A. Moreo, N. Furukawa, E. Dagotto, Phys. Rev Lett. **80**, 845 (1998).
11. E. Dagotto, S. Yunoki, A.L. Malvezzi, A. Moreo, J. Hu, S. Capponi, D. Poilblanc, N. Furukawa, Phys. Rev. B **58**, 6414 (1998).
12. E. Dagotto, S. Yunoki, A. Moreo, `cond-mat/9809380`.
13. A. Moreo, S. Yunoki, E. Dagotto, Science **283**, 2034 (1999).
14. A.J. Millis, P.B. Littlewood, B.I. Shraiman, Phys. Rev. Lett. **74**, 5144 (1995).
15. S.K. Sarker, J. Phys.: Cond. Matter **8**, L515 (1996).
16. H. Röder, J. Zang, A.R. Bishop, Phys. Rev. Lett. **76**, 1356 (1996).
17. D.P. Arovas, G. Gomes-Santos, F. Guinea, Phys.Rev. B **59**, 13569 (1999).
18. D.I. Golosov, M.R. Norman, K. Levin, Phys. Rev. B **58**, 8617 (1998).
19. Y. Liu, J. Dong, D.Y. Xing, Eur. Phys. J. B **3**, 185 (1998).
20. H.C. Ren, M.K. Wu, Phys. Rev. B **58**, 15440 (1998).
21. R. Maezono, S Ishihara, N. Nagaosa, Phys. Rev. B **57**, R13993 (1998), *ibid.* B **58**, 11583 (1998).
22. S. Okamoto, S. Ishihara, S. Maekawa, `cond-mat/9902266`.
23. S. Ishizaka, S. Ishihara, Phys. Rev. B **59**, R8375 (1999).
24. G.S. Uhrig, R. Vlaming, Ann. Physik **4**, 778 (1995).
25. W. Metzner, D. Vollhardt, Phys. Rev. Lett. **62**, 324 (1989).
26. E. Müller-Hartmann, Z. Phys. B **74**, 507 (1989); *ibid.* B **76**, 211 (1989).
27. D. Vollhardt, in *Correlated Electron Systems*,edited by V.J. Emery, (World Scientific, Singapore, 1993) p. 57.
28. A. Georges, G. Kotliar, W. Krauth, M.J. Rozenberg, Rev. Mod. Phys. **68**, 13 (1996).
29. N. Furukawa, J. Phys. Soc. Jpn **63**, 3214 (1994); *ibid.* **64**, 2734, 2754, 3164 (1994).
30. N. Furukawa, `cond-mat/9812066`.
31. D.M. Edwards, A.E.M. Green, K. Kubo, J. Phys.-Cond. Matter **11**, 2791 (1999).
32. B.M. Letfulov, Eur. Phys. J. B **4**, 195 (1998).
33. B.M. Letfulov, Fiz. Tv. Tela (USSR) **19**, 991 (1977).
34. P.-G. de Gennes, J. Friedel, J. Phys. Chem. Solids **4**, 71 (1958).
35. M.E. Fisher, J.S. Langer, Phys. Rev. Lett. **20**, 665 (1968).
36. U. Brandt, C. Mielsch, Z. Phys. B **79**, 295 (1989).
37. U. Brandt, C. Mielsch, Z. Phys. B **75**, 365 (1989).
38. H. Röder, R.R.P. Singh, J. Zang, Phys. Rev. B **56**, 5084 (1997).
39. P. Horsch, J. Jaklič, F. Mack, Phys. Rev. B **59**, R14 (1999).
40. M.J. Calderon, L. Brey, Phys. Rev. B **58**, 3286 (1998).
41. P. Wurth, E. Müller-Hartmann, Eur. Phys. J. B **5**, 403 (1998).
42. P.B. Visscher, Phys. Rev. B **10**, 943 (1974).
43. E.L. Nagaev, Physics-Uspekhi **39**, 781 (1996).
44. M.Yu. Kagan, D.I. Khomskii, M. Mostovoy, Eur. Phys. J. B **12**, 217 (1999).
45. C. Lacroix, Solid St. Comm. **54**, 991 (1985).